Optics Letters

Fiber-optic radio frequency transfer based on passive phase noise compensation with frequency dividing and filtering

RUI HUANG,[1] GUILING WU,[1,2,*] HONGWEI LI,[1] AND JIANPING CHEN[1,2]

[1] *State Key Laboratory of Advanced Optical Communication Systems and Networks, Department of Electronic Engineering, Shanghai Jiao Tong University, Shanghai 200240, China*
[2] *Shanghai Key Laboratory of Navigation and Location-Based Services, Shanghai 200240, China*
**Corresponding author: Guilingwu@sjtu.edu.cn*

Received 27 November 2015; revised 23 December 2015; accepted 24 December 2015; posted 24 December 2015 (Doc. ID 254657); published 1 February 2016

In this Letter, a passive phase noise compensation-based fiber-optic frequency transfer scheme with frequency dividing and filtering is proposed. The probe signal is divided at the remote site and effectively discriminated from the backscattering noises by electrical bandpass filtering at the local site. By combining the bidirectional transmission with the same wavelength on a single fiber, the scheme can reach the maximum bidirectional propagation symmetry and effectively suppress the effect of backscattering at the same time. The proposed scheme is experimentally demonstrated and compared with the scheme with backscattering. The relative frequency stabilities of 3.9×10^{-14}/s and $1.2 \times 10^{-16}/10^4$ s are reached for 40 km transfer, which obviously outperform the scheme with backscattering, especially in terms of short-term stability, and are closed to the floor of the back-to-back experimental system.

OCIS codes: (060.2360) Fiber optics links and subsystems; (060.5625) Radio frequency photonics; (120.3940) Metrology.

http://dx.doi.org/10.1364/OL.41.000626

Many applications such as the comparison of atomic clocks, very long baseline interferometers, and navigation require high-stable dissemination of radio-frequency (RF) [1]. The stability of conventional frequency transfer based on satellite is limited to $\sim 10^{-15}$ at an averaging time of 10^5 s for multipath effects and delay fluctuations caused by troposphere and ionosphere [2]. Taking advantages of wide bandwidth, low attenuation and better reliability, fiber-optic frequency transfer has been considered as a promising way to reach higher stability and long distance. The cancellation of phase fluctuations induced by the temperature variation and mechanical vibration of fiber links is one of the critical issues in the fiber-optic frequency transfer. Active phase noise compensation schemes have commonly been applied, which dynamically measure the round-trip phase fluctuations and, accordingly control tunable phase compensators in the optical domain and/or the electrical domain to cancel the phase fluctuations [3–8]. The feedback loop control-based active schemes, however, require high-precise phase error measurement, fast and large range compensators, and corresponding feedback control algorithms. These make the system become complex and need a longer phase recovery time after a fast link delay perturbation [9,10]. Recently, a passive phase-conjugation compensation scheme based on frequency mixing has been proposed. Several varieties [9–14] have been demonstrated to improve system performance and simplify system structure. Most of them employed WDM-based bidirectional transmission to suppress the effect of backscattering noise [9–13]. The WDM-based transmission, however, suffers from the asymmetry of delay fluctuations for employing different wavelengths, which will degrade the long-term stability of frequency transfer links [15]. Yu *et al.* have proposed a fiber-based stable radio frequency transfer system using a hybrid frequency modulation scheme [16], where the probe signal and the delivered one are combined to modulate the same optical carrier and reflected back directly in the optical domain from the remote site. The scheme simplifies system structure and has better bidirectional symmetry. However, since the forward and backward probe signals have the same RF frequency and are transmitted on the same optical carrier, the backscattering originating from local optical source will not be able to be removed, which will affect the short-term stability of frequency transfer.

In this Letter, we propose a passive phase noise compensation based fiber-optic frequency transfer scheme with dividing and filtering. The same wavelengths are employed in two directions. The probe signal is divided at the remote site before being sent back. The round-trip probe signal is extracted by electrical filtering at the local site to pre-compensate the phase drift of delivered RF signal induced by fiber delay fluctuations via phase-conjugate frequency mixing. In this way, the symmetry of bidirectional transmission is guaranteed, and the effect of backscattering can also be effectively suppressed at the same time.

Figure 1 illustrates the diagram of the proposed passive phase compensation-based fiber-optic frequency transfer

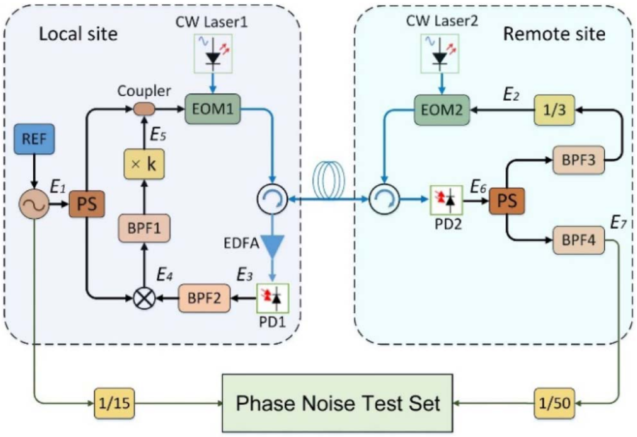

Fig. 1. Schematic of the proposed phase noise compensation system. EOM, electro-optic modulator; EDFA, erbium-doped fiber amplifier; BPF, bandpass filter; PD, photodetector; PS, power splitter.

scheme with dividing and filtering. At the local site, the standard RF signal is split into two branches by a power splitter (PS). One branch is transmitted to the remote site as a probe signal by coupled with the delivered RF signal together and modulated on a single optical carrier. At the remote site, the photodetected signal is split into corresponding bandpass filters (BPF) to discriminate the delivered signal and probe signal, respectively. The delivered signal is provided to users, while the probe signal is divided by 3 and sent back to the local site by modulated on the same optical wavelength as the forward one. The returned signal at the local site is detected by a photodetector (PD) and goes through an electrical BPF to get a cleared round-trip probe signal. The cleared round-trip probe signal is then mixed with the standard RF signal on the other branch to generate the phase pre-compensated RF signal, which is then multiplied by k to obtain the delivered RF signal.

The standard signal at the local site can be denoted as

$$E_1 = \cos(\omega_s t + \varphi_s), \tag{1}$$

where ω_s and φ_s represent the angular frequency and initial phase of the signal, respectively.

At the remote site, the received probe RF signal after the BPF 3 and 1/3 frequency divider can be expressed as

$$E_2 = \cos[(\omega_s t + \varphi_s + \varphi_{\mathrm{FP}})/3], \tag{2}$$

where φ_{FP} is the phase corresponding to the forward fiber link propagation delay, which varies with the thermal and mechanical fluctuations of the fiber link during the forward transmission, and is related to the wavelength of optical carrier.

The signal detected by the PD1 at the local site can be written as

$$\begin{aligned} E_3 = {} & \cos[(\omega_s t + \varphi_s + \varphi_{\mathrm{FP}} + \varphi_{\mathrm{BP}})/3] \\ & + \cos(\omega_s t + \varphi_s + \varphi_{\mathrm{rand1}}) \\ & + \cos[2k(\omega_s t + \varphi_s - \varphi_{\mathrm{FP}}/2 - \varphi_{\mathrm{BP}}/2)/3 + \varphi_{\mathrm{rand2}}] \\ & + \cos[(1 \pm 1/3)\omega_s t + \varphi_{\mathrm{sum1}}] \\ & + \cos[(2k \pm 1)\omega_s t/3 + \varphi_{\mathrm{sum2}}] + \ldots, \end{aligned} \tag{3}$$

where φ_{BP} indicates the phase induced by the backward fiber link propagation delay. The second term on the right-hand side denotes the backscattering noise resulting from the forward transmitted probe signal; φ_{rand1} is its accumulated phase at the local site. The third term is the backscattering noise originating from the delivered RF signal [see Eq. (5)]. The fourth and fifth terms are beat noises between the probe signal and the above two backscattering noises, respectively. φ_{sum1} and φ_{sum2} are the corresponding phases. The rest terms denoted by suspension points include all other high-order beat noises and harmonics.

Since the dominant noises in Eq. (3) have different frequencies with the probe signal ($\omega_s/3$) when k is larger than 1, the noises can be removed by the electrical filter of BPF2. Furthermore, when the forward and backward transmissions employ the same optical wavelengths and the fluctuation of fiber link delay is slow as usual, we have $\varphi_{\mathrm{FP}} = \varphi_{\mathrm{BP}} = \varphi_P$. Hence, the signal after BPF 2 can be expressed as

$$E_4 = \cos[(\omega_s t + \varphi_s + 2\varphi_P)/3]. \tag{4}$$

E_4 is mixed with the standard signal E_1 on the other branch of PS to generate the phase-conjugated signal after BPF1, which is then multiplied by k to obtain the delivered RF signal:

$$E_5 = \cos[2k(\omega_s t + \varphi_s - \varphi_P)/3]. \tag{5}$$

The signals recovered by PD2 at the remote site can be expressed as

$$\begin{aligned} E_6 = {} & \cos(\omega_s t + \varphi_s + \varphi_P) + \cos[2k(\omega_s t + \varphi_s)/3] \\ & + \cos[(\omega_s t + \varphi_s + \varphi_P)/3 + \varphi_{\mathrm{rand3}}] \\ & + \cos[(1 \pm 1/3)\omega_s t + \varphi_{\mathrm{sum3}}] \\ & + \cos[(2k \pm 1)\omega_s t/3 + \varphi_{\mathrm{sum4}}] \\ & + \sum_{m=1}^{3}\sum_{n=1}^{3} \cos((2kn/3 \pm m)\omega_s t + \varphi_{\mathrm{sum\_}mn}). \end{aligned} \tag{6}$$

In Eq. (6), the first two terms on the right-hand side represent the desired probe signal and delivered signal, respectively. The third term is the backscattering noise originating from the backward transmitted probe signal. The next two terms represent the beat noises between the first two terms and the backscattering noise, respectively. The sixth term stands for the beat noise among the first two terms and their harmonics generated mainly in electro-optic modulation and photodetection processes. Consider the power of harmonics decrease with order; we only take the first three order harmonics of the two forward signals.

Table 1 summaries the desired signals and noises recovered by PD1 and PD2 for different k, according to Eqs. (3) and (6). The bold value significance for Table 1 stands for the unfilterable noises whose frequency are the same as the desired signals. One can see that as long as k is larger than three, there will be no dominant noises with the same frequencies as those (ω_s and $2k\omega_s/3$) of desired signals at the remote site and no dominant noises with the same frequency as that ($\omega_s/3$) of desired probe signal at the local site. Therefore, the effect of backscattering and harmonic noises can be efficiently suppressed by employing a k of larger than 3 and suitable BPFs at the both sites. It is worth noting that there exists beating noise between receiving and backscattering optical carriers, which is centered at zero for the same wavelengths at the two sites and has a spectral width of about twice the laser linewidth [17,18]. Obviously, the beating

Table 1. Desired Signals and Noises Recovered by PD1 and PD2 for Different *k*

k	PD2 Signals (ω_s)	PD2 Noises (ω_s)	PD1 Signals (ω_s)	PD1 Noises (ω_s)
1	1, 2/3	1/3, **2/3**, **1**, 4/3, 5/3, 7/3, 8/3, 3, 10/3, 11/3, 4, 13/3, 5	1/3	**1/3**, 2/3, 1, 4/3,
2	1, 4/3	1/3, 2/3, **1**, **4/3**, 5/3, 2, 7/3, 3, 10/3, 11/3, 13/3, 14/3, 5, 17/3, 6, 7	1/3	2/3, 1, 4/3, 5/3
3	1, 2	1/3, 2/3, 4/3, 5/3, 7/3, **1**, **2**, 3, 4, 5, 6, 7, 8, 9	1/3	2/3, 1, 4/3, 5/3, 2, 7/3
4	1, 8/3	1/3, 2/3, 4/3, 5/3, 7/3, 3, 10/3, 11/3, 13/3, 14/3, 5, 17/3, 6, 19/3, 7, 22/3, 25/3, 9, 10,11	1/3	2/3, 1, 4/3, 7/3, 8/3, 3
5	1, 10/3	1/3, 2/3, 4/3, 7/3, 3, 11/3, 13/3, 14/3, 16/3, 17/3,19/3, 7, 23/3, 8, 26/3, 9, 29/3, 11,12, 13	1/3	2/3, 1, 4/3, 3, 10/3, 11/3

noise can also be removed by the BPFs after PDs. A stable RF signal can be obtained after BPF4 at the remote site:

$$E_7 = \cos[2k(\omega_s t + \varphi_s)/3]. \tag{7}$$

The experiment based on the schematic diagram shown in Fig. 1 is demonstrated. The standard RF signal at 300 MHz is generated by a frequency multiplier with an input of 10 MHz reference (Oscilloquartz SA OCXO 8607). The CW lasers at two sites operate at the same wavelength of 1550.10 nm. The RF signals are carried on the optical carriers by a 10 Gb/s LiNbO3 Mach–Zehnder modulator (MZM) biased at the quadrature, and recovered by a 1.2 GHz PD at each site. Each of the applied BPFs has a 3 dB bandwidth of 10 MHz and over 60 dB stopband rejection. The central frequency of BPF 2 is set as 100 MHz. The cleared round-trip probe signal of 100 MHz is mixed with the other part of the standard signal through a mixer with a 60 dB suppression ratio of second-order harmonic of 100 MHz input to generate a 200 MHz phase-conjugation signal after BPF1. The 200 MHz phase-conjugation signal is then multiplied by 5 to produce the 1 GHz delivered signal.

For comparison, the frequency transfer scheme suffering from backscattering is also demonstrated and measured. In the comparison scheme, the same 300 MHz standard signal and 1 GHz delivered RF signal is combined and transferred to the remote site by modulated on a single optical carrier. At the remote site, part of the arrived light is amplified by an EDFA and then directly transferred back to fulfill the round-trip phase noise detection. The other part of light is detected by a PD and then filtered by a BPF to extract the delivered RF signal. At the local site, the round-trip light signal is received by a PD. After a BPF filter at 300 MHz, the recovered RF signal is then divided by 3 to 100 MHz and mixed with the local standard signal to generate a 200 MHz compensated phase conjugation signal. The pre-compensated signal is also multiplied by 5 to produce the 1 GHz delivered RF signal. Because the forward and backward probe signals have the same frequency and are carried on the same wavelength, the effect of backscattering cannot be avoided. Same link configurations, optical and electrical devices, including the lasers, MZM, fiber, PD, BPFs, and mixer, are employed for the proposed and comparison experimental setups.

In each scheme, the standard signal and the received stable signal at the remote site are divided to 20 MHz, which are then input to a phase noise test set (Symmetricom, Inc., TSC5120A) to evaluate the performance of corresponding frequency transfer scheme.

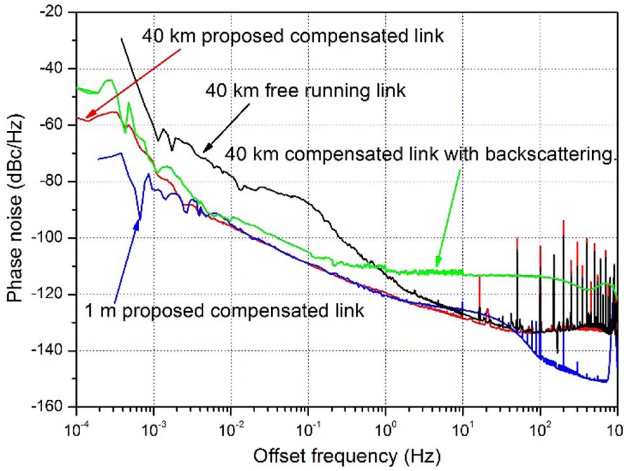

Fig. 2. Measured phase noise spectra of fiber-optic frequency transfer in different system configurations: 40 km free running link, 1 m and 40 km proposed compensated links, 40 km compensated link with backscattering.

Figure 2 shows the measured phase noise spectra of the frequency transfer in different system configurations. All measurements are carried out in an ordinary air-conditioned room with a temperature fluctuation of 3°C. The result over 1 m fiber gives the floor of our experimental system, which is mainly determined by RF signal processes and optical modulation and detection at the two sites. One can see that phase noise of the 40 km free running link is significantly higher than the floor at the offset frequency of less than 1 Hz for the fluctuation of fiber delay mainly induced by temperature variation. The phase noises of the two 40 km compensated links within 0.1–0.001 Hz are almost equal to that of 1 m back-to-back link since both of the schemes can efficiently suppress the lower frequency phase noise induced by the fiber link temperature variation (about 18 dBc/Hz at 0.01 Hz and 22 dBc/Hz at 0.1 Hz, respectively). However, we can see that the phase noise of the 40 km compensated link with backscattering after 0.1 Hz is significantly degraded by the backscattering in the fiber. The phase noise becomes larger than that of the 40 km free running link after about 1 Hz since the effect of backscattering has overwhelmed that of passive phase compensation. On the other hand, the phase noise of the 40 km proposed compensated link is still lower than that of the 40 km free running link and closed to the floor until about 50 Hz. This is because the impact of backscattering is effectively removed in the proposed scheme. The overlap of the phase noise curves of 40 km compensated link, 1 m back-to-back link and 40 km free funning link at about 5–50 Hz offset frequency, may mainly be attributed to the laser FM noise and relative intensity noise (RIN) which

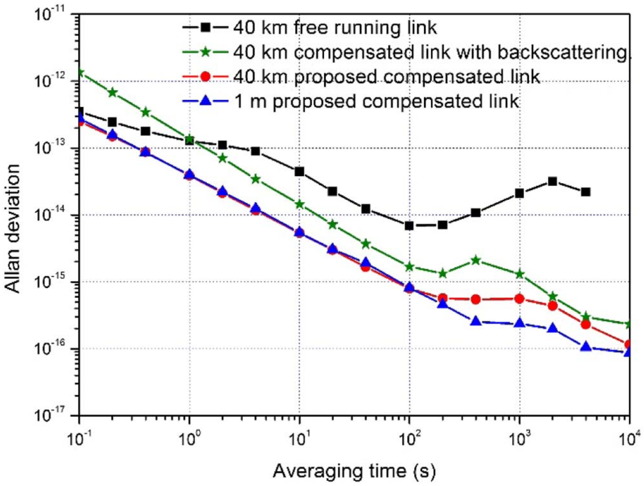

Fig. 3. Fractional instability of different frequency transfer links: 40 km free running link, 1 m and 40 km proposed compensated links, and 40 km compensated link with backscattering.

will result in phase noises during photodetection. After 100 Hz, the 1 m back-to-back link has better performance than the 40 km free running and proposed compensated links. It may be because the two latter links have a lower (more than 12 dB) input optical power for the EDFA before the PD1 than that in the 1 m back-to-back link and suffer from more serious amplified spontaneous emission (ASE) noise, which is mainly in higher frequency [4].

The fractional instability of the different frequency transfer links with a 5 Hz measurement bandwidth in terms of Allan deviation is illustrated in Fig. 3. Compared with the 40 km free running fiber link, both the 40 km proposed compensated link and 40 km compensated link with backscattering have a stabilities decreasing over the averaging time as τ^{-1} and can reach obviously better long-term stabilities close to $1 \times 10^{-16}/10^4$ s. This indicates that both schemes can efficiently compensate for low frequency noises induced by fiber links. The apophysis on Allan deviation curves of each compensated link during around 200–1000 s is mainly attributed to the residual phase noise introduced by the out-of-compensation loop part. The temperature variation period is about 1 h in the experimental room with air-conditioning. Generally, the delay fluctuation related to the out-of-loop components (e.g., optical fiber, electrical cable, and lasers) with the environmental temperature will result in a heave around 200 s–1000 s. Moreover, we can see that the 40 km proposed compensated link can also improve the short-term stability compared with the free running link, from about 1.5×10^{-13}/s to 3.9×10^{-14}/s. In contrast, the short-term stability of 40 km compensated link with backscattering may become worse than that of the free running link, from about $3.5 \times 10^{-13}/0.1$ s to $1.5 \times 10^{-12}/0.1$ s. This is reasonable since the backscattering noise mainly affects the short-term stability. One can also see that the stability of the 40 km proposed compensated link always outperforms those of the other two 40 km links, and almost completely overlaps with the floor of the 1 m compensated link, especially in 0.1 s-100 s. This indicates that the performance of the 40 km proposed compensated link is mainly limited by the experimental system floor, which can be improved by employing high performance optical and RF devices, and precise temperature control of two sites.

In summary, we have proposed a passive phase noise compensation scheme for stable RF frequency transfer. The scheme employs the same wavelengths for the forward and backward transmissions to guarantee the symmetry of bidirectional propagation. Through dividing the probe signal at the remote site and filtering it in the electrical domain at the local site, the impact of backscattering is effectively suppressed at the same time. Frequency transfer over a 40 km optical fiber link based on the proposed scheme is experimentally demonstrated and compared with the scheme with backscattering. The results validate that the proposed scheme can improve the stability of the passive compensated link by efficiently removing backscattering, especially the short-term stability. The reached stabilities, 3.9×10^{-14}/s and $1.2 \times 10^{-16}/10^4$ s, are mainly limited by the system floor.

Funding. National Natural Science Foundation of China (NSFC) (61127016, 61535006); Specialized Research Fund for the Doctoral Program of Ministry of Education of the People's Republic of China (20130073130005).

REFERENCES

1. S. M. Foreman, K. W. Holman, D. D. Hudson, D. J. Jones, and J. Ye, Rev. Sci. Instrum. **78**, 021101 (2007).
2. D. Piester and H. Schnatz, QUEST (Centre for Quantum Engineering and Space-Time Research) at the PTB, PTB-Mitteilungen **119**, 33 (2009).
3. O. Lopez, A. Amy-Klein, C. Daussy, C. Chardonnet, F. Narbonneau, M. Lours, and G. Santarelli, Eur. Phys. J. D **48**, 35 (2008).
4. J. Shen, G. Wu, L. Hu, W. Zou, and J. Chen, Opt. Lett. **39**, 2346 (2014).
5. A. Zhang, Y. Dai, F. Yin, T. Ren, K. Xu, J. Li, Y. Ji, J. Lin, and G. Tang, Opt. Lett. **38**, 2419 (2013).
6. Ł. Sliwczynski, P. Krehlik, Ł. Buczek, and M. Lipinski, IEEE Trans. Instrum. Meas. **60**, 1480 (2011).
7. M. Fujieda, M. Kumagai, T. Gotoh, and M. Hosokawa, IEEE Trans. Instrum. Meas. **58**, 1223 (2009).
8. B. Wang, C. Gao, W. L. Chen, J. Miao, X. Zhu, Y. Bai, J. W. Zhang, Y. Y. Feng, T. C. Li, and L. J. Wang, Sci. Rep. **2**, 556 (2012).
9. J. Wei, F. Zhang, Y. Zhou, D. Ben, and S. Pan, Opt. Lett. **39**, 3360 (2014).
10. F. Yin, A. Zhang, Y. Dai, T. Ren, K. Xu, J. Li, J. Lin, and G. Tang, Opt. Express **22**, 878 (2014).
11. Y. He, B. J. Orr, K. G. Baldwin, M. J. Wouters, A. N. Luiten, G. Aben, and R. B. Warrington, Opt. Express **21**, 18754 (2013).
12. Z. Wu, Y. Dai, F. Yin, K. Xu, J. Li, and J. Lin, Opt. Lett. **38**, 1098 (2013).
13. W. Li, W. T. Wang, W. H. Sun, W. Y. Wang, and N. H. Zhu, Opt. Lett. **39**, 4294 (2014).
14. J. Wei, F. Zhang, S. Pan, and L. Yu, *10th European Microwave Integrated Circuits Conference (EuMIC)* (IEEE, 2015) p. 425.
15. L. Yu, R. Wang, L. Lu, Y. Zhu, J. Zheng, C. Wu, B. Zhang, and P. Wang, Opt. Express **23**, 19783 (2015).
16. L. Yu, R. Wang, L. Lu, Y. Zhu, C. Wu, B. Zhang, and P. Wang, Opt. Lett. **39**, 5255 (2014).
17. P. Gysel and R. K. Staubli, J. Lightwave Technol. **8**, 561 (1990).
18. Ł. Śliwczyński, P. Krehlik, and M. Lipiński, Meas. Sci. Technol. **21**, 075302 (2010).